American Mineralogist, Volume 91, pages 1125–1133, 2006

On the structure of palygorskite by mid- and near-infrared spectroscopy

Vassilis Gionis,[1] George H. Kacandes,[2] Ioannis D. Kastritis,[2] and Georgios D. Chryssikos[1,*]

[1]Theoretical and Physical Chemistry Institute, National Hellenic Research Foundation, 48 Vass. Constantinou Avenue, Athens 11635, Greece
[2]Geohellas S.A., 60 Zephyrou Street, Athens, 17564, Greece

Abstract

The OH-structural characteristics of an iron-rich palygorskite from Western Macedonia, Greece (Gr-1) and an aluminous palygorskite from Florida (PFl-1) were examined by combined Fourier-transform near-infrared reflectance (NIR) and mid-infrared attenuated total reflectance (ATR) spectroscopy. Analyses of samples heated from ambient to 130 °C allowed for the development of a self-consistent set of band assignments for the structural and surface OH and H_2O species of both the hydrated and dehydrated forms. The inner octahedral sites of both samples are largely accounted for by dioctahedral AlAlOH, $AlFe^{3+}OH$, and $Fe^{3+}Fe^{3+}OH$ pairs. Band intensities for these pairs are consistent with variations in the concentration of octahedral Fe and Al in the two samples. In addition, both samples display a trace trioctahedral signature in NIR, which may be related to local trioctahedral domains, or the presence of sepiolite in trace amounts, or as intergrowths. A surface H_2O species typical of the hydrated phase was identified via its NIR combination mode at 5317 cm^{-1}. The desorption of this species by heating revealed distinct silanol groups with overtone and combination modes at 7255 and 4575 cm^{-1}, respectively. Mg-coordinated and zeolitic H_2O species are strongly coupled in the hydrated phase and give rise to NIR combination modes at 5190 and 5240 cm^{-1}. The removal of zeolitic H_2O causes the blue shift of the three dioctahedral OH overtones by ca. 20 cm^{-1} and the rearrangement of the coordinated H_2O manifested by the growth of sharp combination modes at ca. 5215 and 5120 cm^{-1}.

Keywords: IR spectroscopy, palygorskite, NIR spectroscopy, Fe-rich, hormite, hydration

Introduction

Palygorskite and sepiolite are clays consisting of modulated 2:1 layers (for a review on their structure, mineralogy, and properties, see Singer 1989). The tetrahedral sheets of palygorskite are continuous, but every two tetrahedral ribbons along the *b* axis (three in sepiolite) exhibit a reversal of the orientation of their apical O atoms. This reversal leads to the periodic interruption of the octahedral sheet, which, unlike that of smectite, becomes discontinuous (Chisholm 1992; Chiari et al. 2003; Giustetto et al. 2004). Overall, the structure of palygorskite is described as consisting of alternating 2:1 "slabs" and open tunnels running along the *c* axis. The chemical formula of palygorskite, $Mg_5Si_8O_{20}(OH)_2(OH_2)_4{\cdot}4H_2O$, describes a trioctahedral structure. Two different types of H_2O residing in the open channels can be identified: "crystalline" or "coordinated" H_2O bonds directly to the exposed Mg ions to fulfill their coordination requirements, whereas "zeolitic" H_2O interacts with both the coordinated H_2O molecules and the tetrahedral sheet. At ambient conditions, physically adsorbed H_2O is also present in variable quantities. The progressive removal of the various types of H_2O is known to lead to significant changes in the palygorskite structure (Hayashi et al. 1969; VanScoyoc et al. 1979; Singer 1989). The first of these events involves the removal of physisorbed and zeolitic H_2O and the reorganization of the remaining crystalline H_2O. At higher temperatures half of the crystalline H_2O is removed, and the structure folds leading to partial collapse of the channels (Kuang et al. 2004).

Palygorskite exhibits low amounts of tetrahedral substitution (Al^{3+} for Si^{4+}), but Al^{3+}, Fe^{3+}, and to a lesser extent Fe^{2+} ions frequently substitute for octahedral Mg^{2+}. Thus, the more general formula $[M^{2+}_{3x+2}M^{3+}_{2(1-x)}\square_{1-x}]Si_8O_{20}(OH)_2(OH_2)_4{\cdot}4H_2O$ describes palygorskite with a variable dioctahedral-trioctahedral character (Galán and Carretero 1999; Chahi et al. 2002).

Infrared spectroscopy is an essential tool for deciphering the structural characteristics of layer silicates (Farmer 1974; Russell et al. 1994). However, octahedral vacancies in dioctahedral systems as well as the degrees of freedom associated with cation substitution often make the assignments of the infrared spectra difficult and impede their quantitative analysis (Petit et al. 1995; Zviagina et al. 2004). Following an early infrared study of palygorskite by Mendelovici (1973), Serna et al. (1977) were able to separate the fundamental vibrations of the structural hydroxyls from those of the crystalline H_2O species by careful drying and deuteration. Three OH stretching bands were observed and attributed to Al_2OH, $AlFe^{2+}OH$, or AlMgOH and $Fe^{2+}Fe^{3+}OH$ or $Fe^{3+}MgOH$, respectively. Thus, these authors concluded that palygorskite is essentially dioctahedral, with Al and Fe in the inner OH-bearing sites, and most of the Mg ions restricted to the outer sites where they bond to crystalline H_2O. These conclusions were not universally adopted in subsequent studies (Khorami et al. 1989; Augsburger et al. 1998).

The NIR study of several clay specimens by Clark et al. (1990) included two palygorskite source clays from Florida (CM46 and PFl-1), which exhibited sharp and well-resolved bands owing to the 2ν mode of the structural hydroxyls. However, subsequent combined mid- and near-infrared studies of PFl-1 by Madejová and Komadel (2001) and Frost et al. (2001) report very

* E-mail: gdchryss@eie.gr

different spectra and disagree on their interpretation.

This overview of the relevant vibrational literature indicates that no universal agreement exists on the cation substitution patterns and OH speciation of palygorskite. In our opinion, this lack of agreement results mostly from the serious overlap between the stretching modes of the many types of structural hydroxyls and H_2O, especially in the spectra of hydrated samples.

The present work provides new vibrational characterization data on palygorskite and emphasizes the speciation of the structural hydroxyls and H_2O as well as the rearrangements associated with the reversible hydration-dehydration of palygorskite. A sample from newly discovered deposits in Greece (Kastritis et al. 2003) is compared to the Clay Minerals Society Source Clay, PFl-1. Non-destructive, attenuated total reflectance (ATR), in the mid-infrared and diffuse reflectance near-infrared (NIR) spectroscopy, is combined. Instead of the more commonly employed peak-fitting procedures, the second derivative formalism is employed to enhance the resolution of the sharp features, especially where these overlap with broad bands.

A structural interpretation consistent with both samples, both ATR and NIR spectral regions and both states of palygorskite hydration is sought. Moreover, we suggest that the periodic constraint of the octahedral sheet and the possibility for variations in the degree of dioctahedral vs. trioctahedral character can make palygorskite an ideal analog for studying more general structural aspects of octahedral substitution in clay minerals.

Materials and methods

The two palygorskite samples investigated were Gr-1, from the Pefkaki deposit of the Ventzia basin, W. Macedonia, Greece, and PFl-1, a Clay Minerals Society Source Clay from Gadsden County, Florida. Near infrared measurements were made on samples ground to less than 250 μm in a Retsch hammer mill. For the X-ray diffraction (XRD) analysis, the samples were ground to less than 10 μm in a McCrone mill for 10 min, using propanol as the milling fluid. Chemical analysis to determine the structural formula of Gr-1 was conducted by inductivelly coupled plasma-mass spectroscopy (ICP-MS), after removal of colloidal iron by the citrate-bicarbonate-dithionite treatment (Mehra and Jackson 1960) and centrifugation to obtain the <2 μm fraction, which, based on XRD, contained only palygorskite.

Samples were dehydrated by heating in air at 130 °C. The same state was reached by evacuation, drying over $CaCl_2/P_2O_5$, dry nitrogen purging, or a combination of the above. Rehydration was achieved by equilibration at ambient conditions overnight ($T = 25 \pm 3$ °C, $RH = 30 \pm 5\%$).

Thermal analysis data were obtained using a thermobalance with infrared emission quartz heaters (KERN RH120-3). The thermobalance operates in the 40–250 °C range with an accuracy of ±1 °C and ±1 mg of sample. A 10 g sample, previously equilibrated to ambient conditions, was spread evenly on the balance pan and covered with a glass fiber filter. The sample was equilibrated first to 40 °C and then progressively in steps to 250 °C. At each set temperature, equilibrium was defined by reaching a $\Delta w/\Delta t$ slope (w = equilibrated weight, t = time) smaller than 0.02 w%/10 min. The data are equivalent to those of a thermogravimetric experiment at a very slow heating rate.

Powder XRD data were obtained using a Thermo ARL diffractometer (Model X'TRA 17) equipped with a Peltier detector and employing Cu$K\alpha$ radiation at 45 kV and 40 mA. The divergence and receiving slits were 0.4 and 0.5 mm, respectively. The scans were conducted from 2 to 70° 2θ using a step of 0.02° 2θ and a counting time of 10 s.

Mid-infrared data (525–4000 cm^{-1}) were obtained on a Fourier transform instrument (Equinox 55 by Bruker Optics) equipped with a single-reflection diamond ATR accessory (DuraSamplIR II by SensIR Technologies). A small quantity of the powdered sample was placed on the diamond element and held in contact by means of a press. Typically, 100-scan spectra were acquired at 4 cm^{-1} resolution with a zero-filling interpolation factor of 2. Under these conditions, the technique offers a signal to noise ratio sufficient for a second derivative analysis at a temporal resolution of ca. 90 s.

The near-infrared (NIR) spectra (3850–12000 cm^{-1}) were measured using a Fourier transform spectrometer (Vector 22N by Bruker Optics) equipped with an external integrating sphere accessory. All spectra were measured against a gold reference. The typical NIR acquisition parameters were identical to those used for the mid-infrared data. The powdered sample was placed directly on the quartz window of the integrating sphere to form a lightly pressed ca. 1 mm thick layer. A special sealing cup was employed to protect dehydrated samples from exposure to the atmosphere. The same device allowed for the introduction of desiccants and purging gases, and was therefore suitable for real time monitoring of both dehydration and rehydration processes.

Results

Chemical analysis

Based on the results of the chemical analysis (Table 1), Gr-1 is an iron-rich palygorskite with the following structural formula per 20 O atoms: $(Si_{7.74}Al_{0.26})(Al_{0.81}Fe_{1.12}Mg_{2.11})_{4.05}Ca_{0.01}Na_{0.15}K_{0.06}O_{20}(OH)_2(OH_2)_4$. Mermut and Cano (2001) reported the chemical analysis of PFl-1. Although a structural formula is not available for this sample owing to impurities, we note that the Al_2O_3 content of PFl-1 is considerably higher than that of Gr-1 (11.13 vs. 6.96%) whereas the Fe_2O_3 content shows an opposite trend (3.74 vs. 10.6%). The iron-rich nature of Gr-1 with respect to other palygorskites is confirmed by comparison to a broad survey by Galán and Carretero (1999), where the most iron-rich sample contains 0.87 Fe per unit formula.

X-ray diffraction

The powder XRD patterns of both PFl-1 and Gr-1 samples are typical of (mostly monoclinic) palygorskite (Fig. 1). These data confirm the presence of smectite in PFl-1, together with minor amounts of quartz, in agreement with Chipera and Bish (2001). Gr-1 contains minor amounts of smectite (14.5 Å, expandable to 17 Å in ethylene glycol) and quartz. Drying the samples at 130 °C results in the expected shift of the smectite reflection, but does not have an effect on the position or the intensity of the XRD peaks of palygorskite.

Equilibrium weight-loss measurements

The equilibrium weights of PFl-1 and Gr-1 palygorskites as a function of temperature in the range 40–250 °C are shown in Figure 2, together with the first derivative of the equilibrium weight vs. temperature. Two weight loss (dehydration) events are observed over this temperature range at 65 ± 5 and 200 ± 5 °C, in agreement with the literature (Guggenheim and Koster van Groos 2001; Kuang et al. 2004). Equilibrium weights are shown normalized to those at 130 °C because near this temperature both samples exhibit a minimum $\Delta w/\Delta T$. With reference to the minimum at 130 °C, the low-temperature process (40–130 °C) corresponds to the uptake of ca. 7.5% water, and the high-tem-

Table 1. Chemical analysis of the major elements of Gr-1

Gr-1	% oxide	SD
SiO_2	58.9	2.4
Al_2O_3	6.96	0.31
Fe_2O_3	10.6	0.4
MgO	10.8	0.4
CaO	<0.1	0.0
Na_2O	0.60	0.03
K_2O	0.36	0.01
TiO_2	0.33	0.01
MnO	0.05	0.01
P_2O_5	0.04	0.01
LOI	12.0	
Total	100.6	

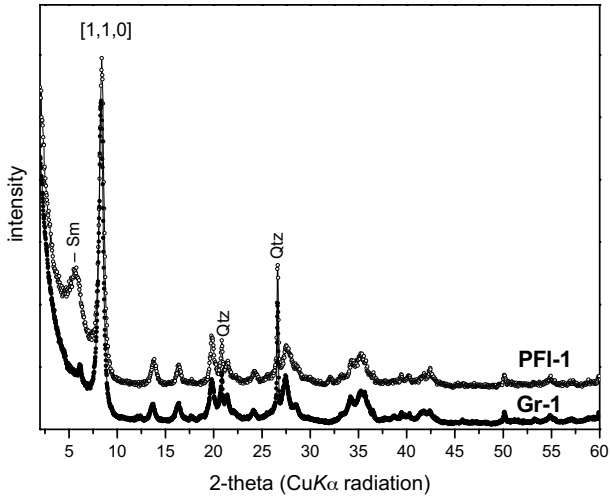

FIGURE 1. Powder XRD spectra (Cu$K\alpha$ radiation) of palygorskites PFl-1 (open circle) and Gr-1 (filled circle).

perature process (130–250 °C) to a loss of ca. 4% water. Hayashi et al. (1969) and Prost (1975) attributed these processes to the removal of four zeolitic and two crystalline H_2O per formula unit, respectively.

In this work, we focus on two quasi-states (ambient and at 130 °C), hereafter referred to as hydrated and dehydrated palygorskite, respectively. These correspond to states I and II of Prost (1975). The as-defined dehydrated form of palygorskite is not the folded structure that forms upon the removal of crystalline H_2O at temperatures greater than ca. 300 °C.

ATR and NIR spectroscopy of hydrated palygorskite

Three frequency ranges of spectral activity are readily discerned in the ATR spectra of Gr-1 and PFl-1 (Fig. 3) at 3700–3000, 1700–1600, and below 1250 cm^{-1}. These are attributed to the stretching OH vibrations of H_2O and structural hydroxyls, the ν_2 bending modes of the various types of H_2O, and the vibrations of the aluminosilicate framework, respectively. The two samples exhibit many similarities in the infrared, best observed by comparing the second derivative spectra (Fig. 3): The bands at ca. 1195 and 640 cm^{-1} were attributed to the asymmetric and symmetric stretching of the Si-O-Si bridges linking the aluminosilicate slabs of palygorskite and sepiolite (Tarte et al. 1973). Their large frequency difference has been related to the large value of this Si-O-Si angle (cf. Chiari et al. 2003; Giustetto et al. 2004). An alternative assignment of the 640 cm^{-1} feature to the δ Mg_3OH vibration of trioctahedral species (Chahi et al. 2002) does not seem to apply in the present case (see below). The bands at ca. 1125, 1090, 1020, and 975 cm^{-1} were attributed to the antisymmetric stretching modes of the tetrahedral silicate sheet (Augsburger et al. 1998). The periodic inversion of the palygorskite/sepiolite tetrahedral sheet shifts the strongest Si-O stretching mode (975 cm^{-1}) to frequencies lower than those observed in smectite (Russell and Fraser 1994). McKeown et al. (2002) performed lattice dynamic calculations to the phyllosilicate ribbons of palygorskite and sepiolite. These authors determined that the 1125 cm^{-1} feature is of A_u symmetry and involves a significant contribution from the Si-O stretching

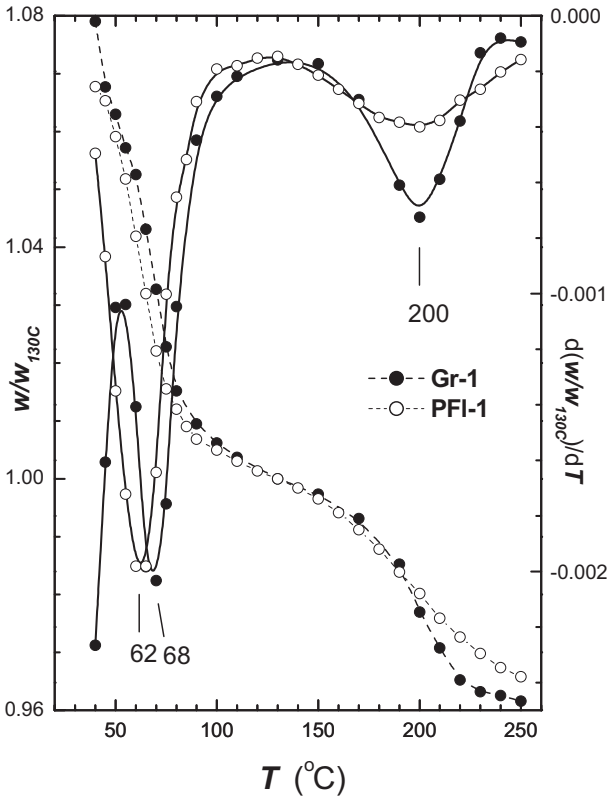

FIGURE 2. Weight loss data of palygorskites PFl-1 and Gr-1. Dashed lines = equilibrium weight normalized to that at 130 °C, and solid lines = first derivative of equilibrium weight vs. temperature.

modes of the linkages connecting the slabs. In addition, they attributed the 1195 and 1090 cm^{-1} bands to stretching and breathing modes of the tetrahedral silicate base.

The two samples exhibit nearly identical ν_2 H_2O triplets at ca. 1675, 1654, and 1625 cm^{-1} (Fig. 3b). However, significant differences are observed in the high frequency part of the spectrum: the second derivative spectrum of PFl-1 shows a strong peak at ca. 3615 cm^{-1}, a weaker peak at 3584 cm^{-1}, and a broader feature at 3544 cm^{-1}. In the corresponding spectrum of Gr-1, the second band is shifted to 3551 cm^{-1} and appears stronger than the 3615 cm^{-1} band (Fig. 3a). In addition, the well-defined AlAlOH deformation mode of the octahedral sheet in PFl-1 (910 cm^{-1}) appears reduced in intensity and at lower frequency (ca. 900 cm^{-1}) than in Gr-1. The latter sample exhibits two additional modes in the MMOH deformation range at 862 and 823 cm^{-1}.

The corresponding NIR spectra (Fig. 4) can also be analyzed in three frequency ranges (Clark et al. 1990). In the 6000–7300 cm^{-1} range, several sharp features are superimposed with a broad and complex envelope of H_2O stretching overtones. In the second derivative spectra, three well-defined features are observed at 7056, 6994, and 6928 cm^{-1}. The former is dominant in the spectrum of PFl-1, but in the case of Gr-1, these are nearly equal in intensity. Both samples exhibit a very weak, but sharp feature at ca. 7215 cm^{-1}, whereas Gr-1 shows also a trace absorption at 7184 cm^{-1}. At intermediate frequencies, (4800–5400 cm^{-1}), absorption in the NIR is dominated by the H_2O combination modes. These are more clearly defined in the second derivative spectrum, where both samples show a triplet of sharp bands at ca. 5320, 5240,

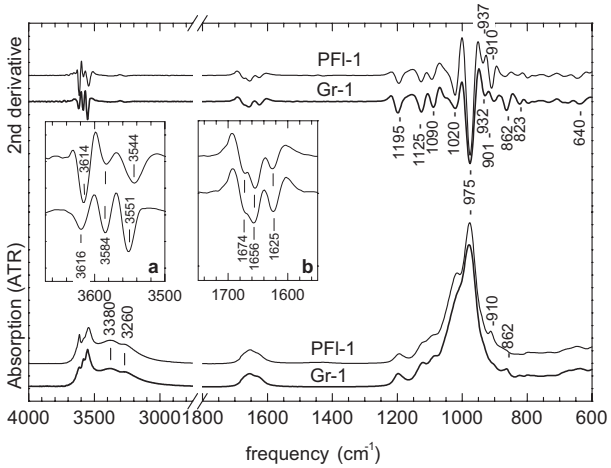

FIGURE 3. Attenuated Total Reflectance infrared spectra of Gr-1 and PFl-1 palygorskites, and their second derivatives. The spectra have been offset for clarity. Insets show in detail the OH stretching (**a**) and H_2O bending (**b**) regions of the second derivative spectra.

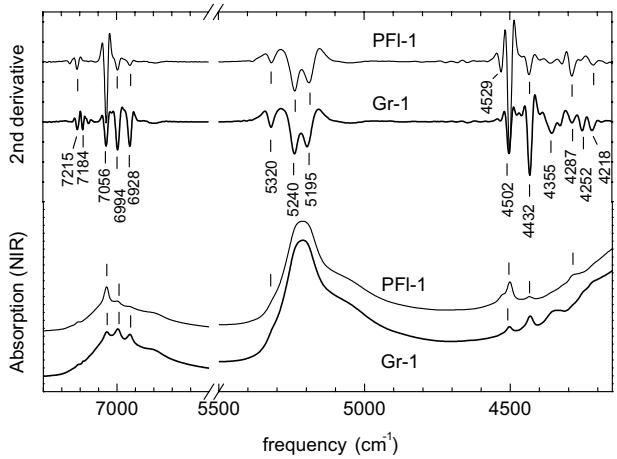

FIGURE 4. Near-infrared absorption spectra of Gr-1 and PFl-1 palygorskites, and their second derivatives. The spectra have been offset for clarity.

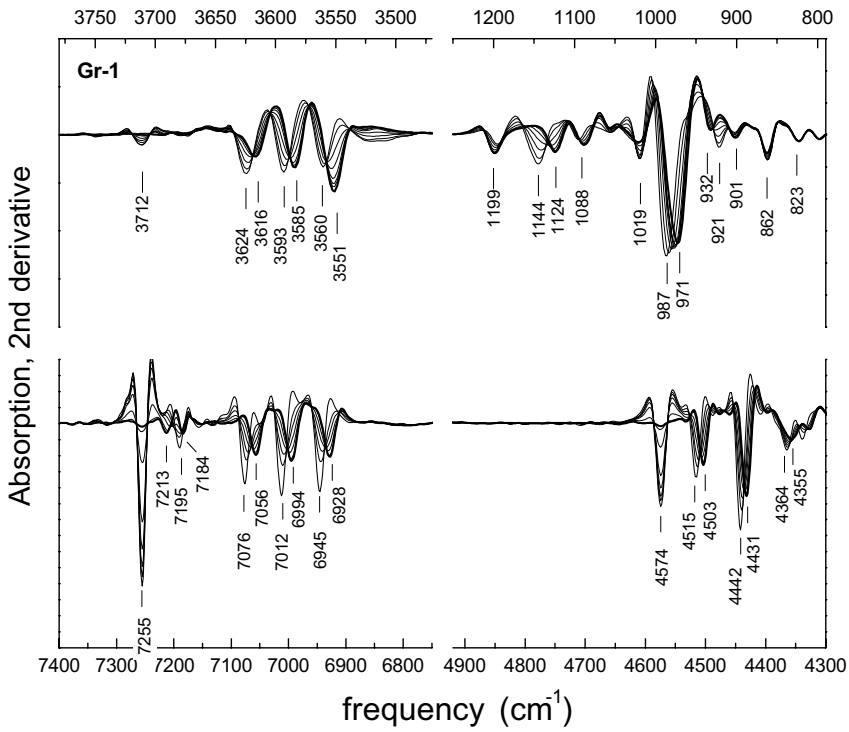

FIGURE 5. Spectral sequence of dehydrated Gr-1 measured upon rehydration at ambient conditions, as seen in the second derivative of its ATR (top) and NIR spectra (bottom).

and 5195 cm^{-1}. Finally, the combination modes of the structural hydroxyl groups, absorbing below 4600 cm^{-1} (Post and Noble 1993), appear substantially differentiated. The spectrum of PFl-1 is dominated by a strong mode at 4502 cm^{-1}, with a shoulder at 4529 cm^{-1}. Weaker sharp bands are observed at 4432, 4287, and 4218 cm^{-1}. These bands can also be observed in the spectrum of Gr-1, with the strongest feature appearing at 4431 cm^{-1}, whereas two new features appear at 4355 and 4252 cm^{-1}.

NIR spectra of PFl-1 were reported previously by Frost et al. (2001) and by Madejová and Komadel (2001). The spectrum reported by Frost et al. is at variance with the data in Figure 4. Frost et al. report the overtone of a structural hydroxyl at 7093 cm^{-1}, and a multiplet at 4503, 4320, 4280, 4102, and 4050 cm^{-1} is attributed to the combination modes of ill-defined terminal hydroxyls (MgOH, AlOH, and FeOH). These discrepancies may be related to errors in the peak-fitting analysis adopted by these authors. Regardless, their assignments are not diagnostic for any of the expected dioctahedral or trioctahedral hydroxyl arrangements of palygorskite. In contrast, the spectrum reported by Madejová and Komadel (2001) is very similar to that shown in Figure 4, but the proposed band assignments are incomplete.

ATR and NIR monitoring of dehydrated palygorskite and its rehydration

Figures 5–7 depict the room-temperature second derivative spectra of dehydrated PFl-1 and Gr-1 as a function of exposure time to ambient humidity. Dehydration has a pronounced effect on the spectra, but is fully reversible within the sensitivity of both ATR and NIR spectroscopies in agreement with Kuang et al. (2004). New bands appear in the spectra of the dehydrated palygorskite at 3712, 4574, and 7255 cm^{-1} (hereafter exact frequencies are given for Gr-1 with reference to Fig. 5). The three sharp high-frequency mid-infrared modes of the hydrated form shift by 8–9 cm^{-1} upon dehydration and appear at 3624, 3593, and 3560 cm^{-1}. The corresponding NIR modes exhibit a parallel shift by 17–20 cm^{-1}, and appear at

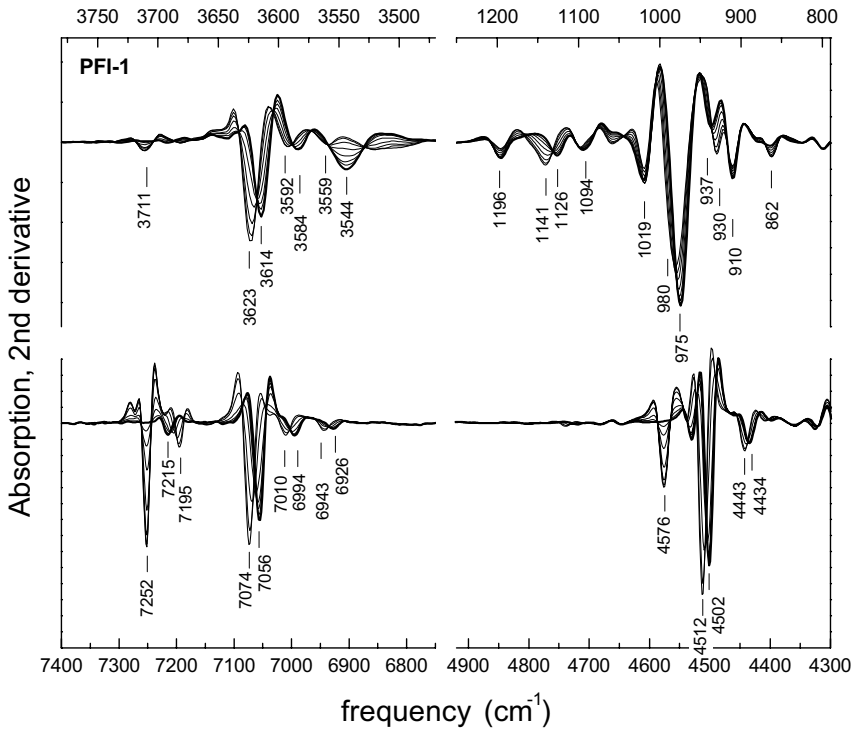

FIGURE 6. Spectral sequence of dehydrated PFl-1 measured upon rehydration at ambient conditions, as seen in the second derivative of its ATR (top) and NIR spectra (bottom).

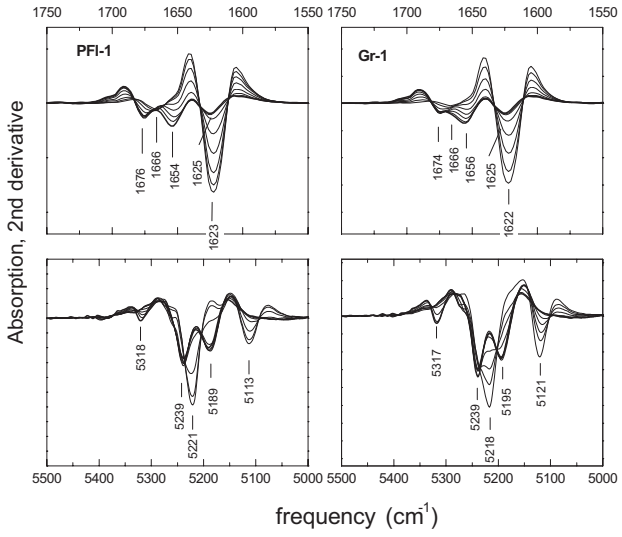

FIGURE 7. Detail of the second derivative spectra over the H_2O bending (ATR, upper) and combination (NIR, lower) ranges, for PFl-1 (left) and Gr-1 (right). The spectral series correspond to the rehydration of dehydrated samples.

7076, 7012, and 6945 cm^{-1} in the dehydrated form. Similarly, dehydration induces the blue-shift of 4431 and 4503 cm^{-1} modes by 11–12 cm^{-1} in both Gr-1 and PFl-1. In addition to these, a weak feature at ca. 7214 cm^{-1}, shifts to ca. 7195 cm^{-1} upon dehydration. The corresponding fundamental of these modes is below the detection limit of the second derivative ATR spectra. In the low-frequency part of the ATR spectrum, dehydration induces the shift of the 1124 and 971 cm^{-1} bands to 1144 and 987 cm^{-1}, respectively. The 932 cm^{-1} feature of Gr-1 appears to shift to 921 cm^{-1}, whereas the corresponding trend for PFl-1 is from 937 to 930 cm^{-1}. No shifts of the 901, 862, and 823 cm^{-1} bands of Gr-1 are observed (910, 862 cm^{-1} for PFl-1).

Dehydrated palygorskite exhibits a very sharp (intense, in the second derivative) bending mode of H_2O at 1622 cm^{-1} (Fig. 7). Weak and broader features are observed at ca. 1666 cm^{-1}. Equally pronounced are the changes in the frequency range of the H_2O combination modes. The high frequency component at 5317 cm^{-1} is absent from the spectra of the dehydrated palygorskites and the doublet at 5239 and 5195 cm^{-1} appears at 5218 and 5121 cm^{-1} upon dehydration.

DISCUSSION

Structural hydroxyls

A good starting point for discussing the OH speciation in palygorskite is the assignment of a well-defined triplet in the high frequency part of the NIR spectrum. Within ±1 cm^{-1}, these bands appear at the same frequencies in both Gr-1 and PFl-1: 7056, 6994, and 6928 cm^{-1} in the hydrated form and 7076, 7012, and 6945 cm^{-1} in the dehydrated form. According to Clark et al. (1990), these bands fall in a range indicative of dioctahedral hydroxyl groups in smectite. Madejová and Komadel (2001) attributed a 7058 cm^{-1} band of PFl-1 to the AlAlOH unit. Note further that the three high frequency bands are equidistant in both the hydrated and dehydrated forms (cf. Gates 2005), and the intensity of the middle component is qualitatively similar to that expected for a mixed ABOH site (A, B are metal ions in a dioctahedral arrangement), where the AAOH and BBOH sites correspond to the highest and lowest frequency components. The situation is remarkably similar to that reported for amphiboles and brucite-like minerals, where Mg^{2+} and Fe^{2+} populate the trioctahedral sites giving rise to a quartet of OH stretching overtones (Clark et al. 1990). We therefore suggest that the high-frequency NIR triplet in palygorskite monitors dioctahedral arrangements populated by two different cations, one of which is Al^{3+}. Based on the results of the chemical analysis, the second octahedral ion ought to be Fe^{3+}.

To test this hypothesis, we seek supporting evidence from the various stretching-bending combinations in the low-frequency part of the NIR spectrum, as well as the high- and low-frequency parts of the mid-infrared spectrum where the fundamental MMOH stretches and the corresponding bending deformation modes are known to be active.

There is ample evidence in the literature that the stretching-bending combination mode of the dioctahedral AlAlOH group in aluminous smectite or kaolin minerals is observed above ca. 4500 cm^{-1}, whereas that of the $Fe^{3+}Fe^{3+}OH$ analog is observed at ca. 4370 cm^{-1} (Clark et al. 1990; Gates 2005, and references

therein). Palygorskites CM46 and PFl-1 exhibit this AlAlOH mode at ca. 4500 cm^{-1}, which is about three times sharper than the corresponding band of montmorillonite (Clark et al. 1990; Madejová and Komadel 2001). Ferruginous smectite and nontronite also exhibit a strong $Fe^{3+}Fe^{3+}OH$ mode at ca. 4370 cm^{-1} (Post and Noble 1993), although minor substitutions of Fe^{3+} by Al^{3+} are reported to give rise to a AlAlOH combination at unusually high frequency (Gates et al. 2002). If these assignments are correct, the combination mode of a mixed-cation $AlFe^{3+}OH$ group, would be expected half way between the AlAlOH and $Fe^{3+}Fe^{3+}OH$ combinations i.e., in the vicinity of 4435 cm^{-1}. The palygorskites investigated here do exhibit sharp combination modes at ca. 4500 and 4430 cm^{-1}, whereas in Gr-1 a weak 4360 cm^{-1} band is also visible. The relative intensities of these three bands are compatible to those of the previously discussed stretching overtones. Finally, the three combination bands appear to shift in a synchronous manner (by +11 cm^{-1}) upon dehydration. As a result, the NIR spectra of the palygorskites investigated here provide evidence for the presence of dioctahedral sites populated by Al^{3+} and Fe^{3+}.

Mid-infrared bands compatible with these assignments can be identified in the second derivative ATR spectra (Fig. 5 and 6). The AlAlOH, $AlFe^{3+}OH$, and $Fe^{3+}Fe^{3+}OH$ stretching vibrations of the hydrated forms are observed at 3615, 3594, and 3551 cm^{-1}, respectively, and shift by ca. +10 cm^{-1} upon dehydration. Note that in PFl-1, the weak $Fe^{3+}Fe^{3+}OH$ stretch is visible only in the spectrum of the dehydrated form because in the hydrated state it is masked by a relatively strong band at 3544 cm^{-1} owing to H_2O (Khorami and Lemieux 1989). The same band biases the relative intensity of the much stronger 3551 cm^{-1} component in the spectrum of ambient Gr-1. The AlAlOH, $AlFe^{3+}OH$, and $Fe^{3+}Fe^{3+}OH$ deformation modes of Gr-1 are observed at 901, 862, and 823 cm^{-1} and do not shift upon dehydration. In PFl-1, the AlAlOH and $AlFe^{3+}OH$ deformation modes appear at 910 and 862 cm^{-1}, respectively, but their $Fe^{3+}Fe^{3+}OH$ counterpart is weak and below the detection limit of our techniques.

The above vibrational assignments (summarized in Table 2) are compatible with several previous studies. Farmer (1974) reported that the fundamental AlAlOH stretch of smectite is observed at 3620–3640 cm^{-1}, and Goodman et al. (1976) attributed a band at 3565 cm^{-1} to the OH stretch in $Fe^{3+}Fe^{3+}OH$. Petit et al. (1995) studied synthetic smectites with variable Al-Fe octahedral occupancy and found evidence for the $AlFe^{3+}OH$ stretch at 3596 cm^{-1}, i.e., at the barycenter of the AlAlOH and $Fe^{3+}Fe^{3+}OH$ modes. Characteristic frequencies for the various deformation modes are reported at 930 (AlAlOH), 873 ($AlFe^{3+}OH$), and 816 cm^{-1} ($Fe^{3+}Fe^{3+}OH$) (Russell et al. 1970; Farmer 1974; Russell and Fraser 1994). Chahi et al. (2002) observed the AlAlOH stretch of palygorskite from Morocco at 3616 cm^{-1}, and the AlAlOH, $AlFe^{3+}OH$ deformations at 911 and 867 cm^{-1}, respectively.

As a direct consequence of this analysis, the participation of bivalent ions (Mg or Fe^{2+}) in the inner octahedra of palygorskite becomes of secondary importance because it was based (Serna et al. 1977; Augsburger et al. 1998; Madejová and Komadel 2001) on features that are now recognized as related to the substitution of Al by Fe^{3+}. Homovalent substitution of Al by Fe^{3+} maintains charge balance and is compatible with the very low cation-exchange capacity of palygorskite. The degree of this substitution is particularly pronounced in Gr-1 in agreement with the results of its chemical analysis.

However, the possibility that the dioctahedral OH groups in palygorskite might coexist with trioctahedral, primarily Mg_3OH, species as in sepiolite cannot be excluded. Hayashi et al. (1969), Serna et al. (1975), and Prost (1975) reported that sepiolite exhibits a sharp Mg_3OH stretch in the 3680–3690 cm^{-1} range, i.e., at slightly higher frequencies than the corresponding mode of talc (3677 cm^{-1}, Farmer 1974) or saponite (3679 cm^{-1}, Madejová 2003). A Moroccan palygorskite was interpreted by Chahi et al. (2002) as having mixed trioctahedral-dioctahedral character because it exhibits a clear Mg_3OH stretch at 3680 cm^{-1}, in addition to the dioctahedral (Al,Fe^{3+}) OH vibrational signature discussed above. Note that the frequency of the Mg_3OH stretch is affected by low-temperature dehydration in sepiolite, but remains unaffected in trioctahedral smectite.

Along these lines we note that the ATR spectra of both PFl-1 and Gr-1 (Figs. 5 and 6) show slight inflections above 3650 cm^{-1}, features that cannot be truly diagnostic for Mg_3OH. However, both samples exhibit low intensity bands in the near-infrared between 7180 and 7220 cm^{-1}, and these bands could be attributed to the stretching overtone of the Mg_3OH species. More

TABLE 2. Summary of the proposed near- and mid-infrared assignments for palygorskite Gr-1 in its ambient and dehydrated (130 °C) forms

Ambient	Dehydrated	Assignment / comments
–	7255	2ν SiOH, outer surface
7213	7195	2ν Mg_3OH, trioct. Pal or Sep
7184	(7184)	2ν Mg_3OH, Sap or Tlc
7056	7076	2ν Al_2OH
6994	7012	2ν $AlFe^{3+}OH$
6928	6945	2ν $Fe_2^{3+}OH$
5317		(ν+δ) H_2O, chemisorbed on SiOH
5239		(ν+δ) H_2O, coordinated and zeolitic
	5218	(ν_a+δ) H_b–OH_a, coordinated
5195*		(ν+δ) H_2O, coordinated and zeolitic
	5121*	(ν_b+δ) H_b–OH_a, coordinated
–	4574	(ν+δ) SiOH, outer surface
4503	4515	(ν+δ) Al_2OH
4431	4442	(ν+δ) $AlFe^{3+}OH$
4355	4364	(ν+δ) $Fe_2^{3+}OH$
–	3712	ν SiOH, outer surface
3616	3624	ν Al_2OH
3585	3593	ν $AlFe^{3+}OH$
3551	3560	ν $Fe_2^{3+}OH$
1674		δ H_2O interacting with SiOH?
1656		δ H_2O physisorbed?
1625		δ H_2O coordinated and zeolitic
	1622	δ H_b–OH_a, coordinated
1199	1195	
1124	1144	
1088*	1091	ν Si-O-Si intra-slab and inter-slab
1019	1019	ν $Si\text{-}O^-$
971*	987*	
932*	921*	
901*	901*	δ Al_2OH
862	862	δ $AlFe^{3+}OH$
823	823	δ $Fe_2^{3+}OH$

Notes: Frequencies are determined from the second derivative spectra.
* Bands that appear shifted by more than ±3 cm^{-1} in the corresponding spectra of palygorskite PFl-1.

specifically, PFl-1 shows a band at 7215 cm^{-1} that shifts upon dehydration to 7195 cm^{-1}. In Gr-1, the same band is observed at 7213 (7190) cm^{-1}, but coexists with another weak feature at 7184 cm^{-1} that is not affected by dehydration. Clark et al. (1990) identified a feature at 7184 cm^{-1} with the overtone of the 3677 cm^{-1} Mg_3OH stretch of talc, and stated that this feature is difficult to distinguish from the analogous modes of hectorite, sepiolite, and saponite. Instead, the overtone of the 3690 cm^{-1} Mg_3OH fundamental of sepiolite SepSp-1 (Frost et al. 2001) is observed as a very strong and sharp band at 7214 cm^{-1} (unpublished results, this laboratory). Based on the above, it is possible to identify the presence of saponite (or talc) in Gr-1 and of Mg_3OH from sepiolite/palygorskite in both PFl-1 and Gr-1. Both minerals/species are detected by high resolution NIR, but fall below the detection limit of both ATR and XRD. Whereas saponite is commonly detected in clay horizons near Gr-1, and may be present in trace amounts in this sample, it is not possible to determine whether the Mg_3OH signature detected in both PFl-1 and Gr-1 is related to an admixture of sepiolite or to a barely detectable amount of hydroxyl groups in a trioctahedral form in palygorskite.

Finally, we comment that the dehydration-induced frequency shifts of the OH modes of PFl-1 and Gr-1 are in disagreement with those reported by Prost (1975) for palygorskite from Seradilla, Spain. Prost determined that the fundamental OH stretching and deformation modes shift upon dehydration by +10 and –10 cm^{-1}, respectively. This shift implies that this palygorskite would exhibit OH combination frequencies independent of hydration. Instead, our data show that only the stretching fundamentals shift by +10 cm^{-1} in excellent agreement with the +10 and +20 cm^{-1} shifts of the combination and overtone modes in the NIR. Further, our data allow for the calculation of the harmonic frequencies and anharmonicity parameters of the structural hydroxyls in palygorskite according to the formalism compiled by Bokobza (2002). The three hydroxyl species, in both samples and in both hydrated and dehydrated forms exhibit remarkably similar anharmonicities and anharmonicity constants (87 ± 1 cm^{-1} and 0.023 ± 0.001, respectively; Table 3). These values fall in the range reported for the OH stretching modes of alunites (Breitinger et al. 1999) and brucite-type hydroxides (Weckler and Lutz 1996).

Surface silanol groups

A prominent NIR manifestation of palygorskite dehydration is the emergence of strong and sharp bands at 7255 (7252) and 4574 (4576) cm^{-1} in the spectra of Gr-1 (PFl-1), i.e., at frequencies higher than those expected for either trioctahedral or dioctahedral structural hydroxyls (Figs. 5 and 6). To assign these bands we correlate their growth with the parallel emergence of a mid-infrared band at 3712 (Gr-1) or 3711 cm^{-1} (PFl-1). Assuming that the 7255 cm^{-1} mode is the overtone of the 3712 cm^{-1} stretch, the estimate of the anharmonicity parameters ($\boldsymbol{X} \approx$ 85 cm^{-1}, $\boldsymbol{x_e} = 0.022$) compare favorably to those of the structural hydroxyls (Table 3).

Serna et al. (1977) identified a 3705 cm^{-1} feature in a dehydrated palygorskite from Georgia, which shifts to 2745 cm^{-1} upon deuteration. The same authors assigned this feature to surface silanol groups by analogy to a similar feature of dehydrated sepiolite (Ahlrichs et al. 1975; Serna et al. 1975). Based on the relatively high frequency of this mode and its response to deuteration, Serna et al. (1977) assumed that the silanol group is isolated, and argued convincingly that this should represent a termination defect along the *c* axis of the crystal. More recently, Kuang et al. (2004) extended the earlier ^{29}Si NMR study of Barron and Frost (1985) and concluded that ca. 8% of the Si nuclei in PFl-1 exist as SiOH.

Relevant comparisons can be made with silanol defects on various types of silica particles, and their role as adsorption centers. Bush et al. (1983) reported that dry silica particles exhibit SiOH stretching and deformation modes at 3750 and 870 cm^{-1}, respectively, whereas the NIR-active combination and overtone modes appear at 4550 and 7326 cm^{-1}. In a similar study of activated aerosil and precipitated types of silica, Morrow and McFarlan (1992) identified two types of SiOH groups. The first type is thought to produce a set of modes (combination, stretching and deformation) at 4510, 3750, and 760 cm^{-1}, whereas the second type displays these modes shifted to 4580, 3740, and 840 cm^{-1}. Szekeres et al. (2003) performed mid-infrared studies of Stöber silica particles at 550 °C and reported the stretching of silanol groups at 3724 cm^{-1}. They further reported that these silanol absorption bands vanish upon washing with water or methanol. This point is advanced further by Yuan et al. (2004), who investigated the surface sites of diatomite. At ambient conditions, silanols in diatomite are hydrogen bonded with surface H_2O and do not exhibit well-resolved bands in the infrared. However, above ca. 200 °C, dehydration occurs and a characteristic SiOH stretch appears at ca. 3740 cm^{-1}. The exact stretching frequency of dehydrated silanol groups is thought to depend on whether these are located on adjacent, distant, or isolated Si centers. Among the various structures of silanol groups proposed by Yuan et al. (2004), Figure 8 shows a structure relevant to palygorskite and compatible to the termination defect hypothesis of Serna et al. (1977). The silanol groups terminate along every other Si atom of the rim running along the *c* axis, and more specifically at the Si4 site according to the atom numbering by Giustetto et al. (2004). As such, the O-O distance of neighboring silanols equals the *c* axis dimension of either unit cell (5.25 Å). Owing to this relatively large distance, the possibility for hydrogen bonding between adjacent silanol groups is negligible, unless it is mediated by a well-defined type of surface-adsorbed H_2O. Should the presence of such a type of H_2O be confirmed in the hydrated state, it could account for the dramatic dependence of the silanol modes on hydration.

TABLE 3. Harmonic frequencies (ν_{harm}), anharmonicities (X), and anharmonicity constants ($x_e = X/\nu_{harm}$) of the OH stretching modes of palygorskite at ambient conditions and after dehydration at 130 °C

assignment	ν_{obs} (cm^{-1})	$2\nu_{obs}$ (cm^{-1})	ν_{harm} (cm^{-1})	X (cm^{-1})	x_e
ambient					
AlAlOH	3615	7056	3789	87.0	0.023
$AlFe^{3+}OH$	3585	6994	3761	88.0	0.023
$Fe^{3+}Fe^{3+}OH$	3551	6928	3725	87.0	0.023
dehydrated					
AlAlOH	3624	7075	3797	86.5	0.023
$AlFe^{3+}OH$	3593	7011	3780	87.5	0.023
$Fe^{3+}Fe^{3+}OH$	3560	6944	3736	88.0	0.023
SiOH	3712	7254	3882	85.0	0.022

Surface, zeolitic, and coordination H_2O

The broad and overlapping nature of the various H_2O stretching modes of palygorskite, and their occurrence in the same frequency range as the (much sharper) structural OH stretching counterparts, limit the usability of the second derivative analysis to regions corresponding to the H_2O bending and stretching-bending combinations. The spectra in Figure 7 complement those in Figures 5 and 6 and illustrate the dehydration-induced changes that are related to the H_2O species in palygorskite. The spectra of H_2O in ambient PFl-1 and Gr-1, as well as their changes upon dehydration, appear very similar to each other, despite the fact that these materials exhibit a drastically different inner octahedral composition (see above). A similar observation can be made on the basis of the mid-infrared spectra of hydrated palygorskites from six different locations by Khorami and Lemieux (1989).

The H_2O bending region of dehydrated Gr-1 and PFl-1 is dominated by a sharp band at 1622 cm^{-1} with a weak and broad shoulder at 1666 cm^{-1}. Similarly, the corresponding combination region is dominated by two well-defined peaks at 5120 and 5220 cm^{-1} (Fig. 7). Mendelovici (1973) studied a Georgian "attapulgite" in its dehydrated state and reported two H_2O stretching modes at 3620–25 and 3520–25 cm^{-1}, and one sharp bending mode at 1625–30 cm^{-1}. A subsequent thorough investigation of a Spanish palygorskite by Prost (1975) confirmed the findings of Mendelovici (1973) and attributed the above mentioned features to H_2O in C_s symmetry coordinated to Mg at external octahedral sites, i.e., chemisorbed at the side walls of the palygorskite/sepiolite channels. Finally, Serna et al. (1977) studied palygorskite after deuterating its structural hydroxyls and reintroducing H_2O, and concluded that there is only one type of coordinated H_2O in the dehydrated state, and that this strongly interacts with the Si-O-Si linkages between the slabs. The extent of this interaction is such that the H_2O stretching modes can be treated as completely decoupled from each other.

Based on the above, the assignment of the H_2O NIR spectrum of dehydrated palygorskite is straightforward. The bands at ca. 5220 and 5120 cm^{-1} are related to a single type of H_2O and represent the combinations of the two decoupled fundamental stretches at ca. 3625 and 3525 cm^{-1} with the bending at 1620 cm^{-1}. The 100 cm^{-1} frequency difference between the two combination modes reflects directly on the (more difficult to observe) splitting of the stretching fundamentals. The exact value (e.g., 108 cm^{-1} in PFl-1 vs. 97 cm^{-1} in Gr-1) could be used to probe subtle structural variations in palygorskite of variable origin.

In contrast, the H_2O spectrum of hydrated palygorskite is considerably more complicated with three bending components in the mid-infrared (1625, 1655, and 1675 cm^{-1}) and three combination bands in the near-infrared (5190, 5240, and 5317 cm^{-1}). The aforementioned bands attributed to H_2O species coordinated to the external Mg ions are not detected in the hydrated sample. This indicates that the interaction between zeolitic and coordinated H_2O in the channels alters drastically the structure of the latter.

In addition, the vibrational signature of H_2O in the hydrated state (Fig. 8) may include contributions from H_2O adsorbed on the surface and in interaction with the silanol groups. Very slow dehydration of Gr-1 over a period of 2 h in the presence of P_2O_5, leads to the intensity increase of the silanol overtone and combination bands at 7255 and 4574 cm^{-1}, respectively (Fig. 9). At these early dehydration stages, the only other spectral change accompanying the growth of silanol bands is the decrease of one H_2O combination component at 5317 cm^{-1}. The bands related to the dioctahedral hydroxyl species and the remaining H_2O combination modes at 5239 and 5195 cm^{-1} remain unperturbed. This indicates that the dehydration of palygorskite (Fig. 6) is a combination of two processes that can now be resolved. Surface dehydration is shown to precede the removal of zeolitic H_2O from the channels. Conversely, the very slow rehydration of dehydrated palygorskite indicates that zeolitic H_2O is admitted in the channels before the surface silanols become hydrated (data not shown).

The above analysis allows for the specific assignment of the 5317 cm^{-1} mode to surface H_2O interacting with the silanol groups, and leaves the remaining modes at 5195 (5189 for PFl-

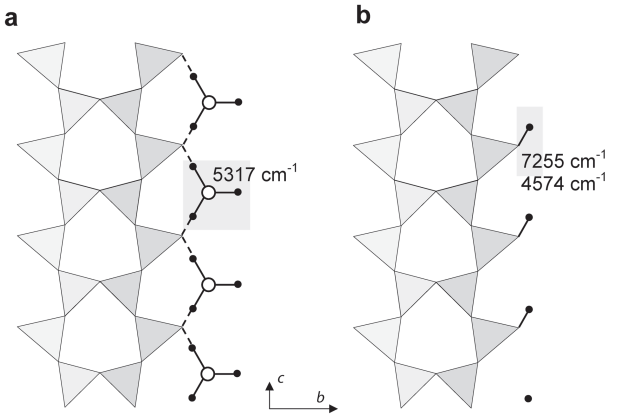

FIGURE 8. Schematic representation of the surface defects in palygorskite. The edge row of silicate tetrahedra is viewed down the *a*-axis and shaded. Chemisorbed H_2O is shown in hydrated palygorskite (**a**), converting to quasi-isolated silanol groups upon dehydration (**b**).

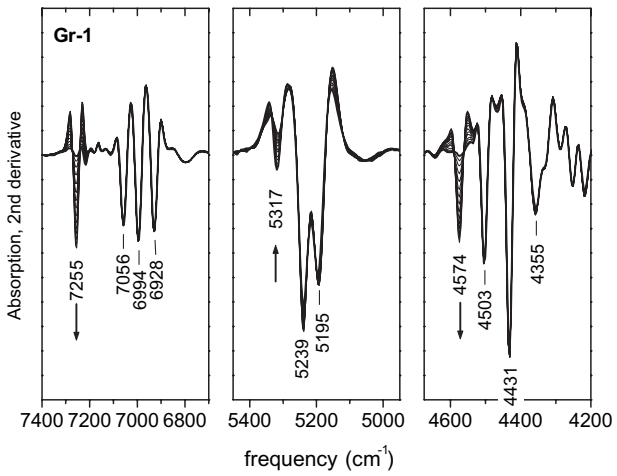

FIGURE 9. NIR spectra of Gr-1 in its early stages of dehydration. The sample had been preheated at 40 °C for 1 h and then measured in real time during dehydration by P_2O_5.

1) and 5239 cm^{-1} to represent the stretching-bending combination modes of interacting coordinated and zeolitic H_2O. Their frequency maxima differ by only about 50 cm^{-1} compared to about 100 cm^{-1} in the dehydrated state, which indicates a more uniform distribution of oscillators. However, a more specific assignment is not straightforward. On one hand, the two combination features could be treated as independent indicators of the two types of H_2O present. In this case, the 5239 cm^{-1} band falls in the range where the sharp combination mode of H_2O in expandable 2:1 phyllosilicates is observed (5230–5260 cm^{-1}, Clark et al. 1990) and could therefore be attributed to zeolitic H_2O in interaction with the tetrahedral sheets. Then, the ca. 5190 cm^{-1} frequency component that shows some dependence on the type of palygorskite should be attributed to the more strongly bound coordinated or crystalline H_2O. In contrast, zeolitic and coordinated H_2O could be viewed as a strongly H-bonded cluster of defined geometry, with vibrational activity depending on both its point group and site symmetry.

ACKNOWLEDGMENTS

The authors acknowledge the kind technical assistance of Y. Yiannopoulos, S. Kemidis, E. Typa, and M. Drossos, and many stimulating discussions with E. Dessipri. We also express our appreciation to the reviewers, Jeffrey Post, Smithsonian Institution, and Ann Hofmeister, Washington University, St. Louis, and to the Associate Editor (Steve Guggenheim, University of Illinois at Chicago) for their very useful comments and suggestions. Research at TPCI/NHRF has been supported by an applied spectroscopy contract with Geohellas SA.

REFERENCES CITED

Ahlrichs, P.A., Serna, C. and Serratosa, J.M. (1975) Structural hydroxyls in sepiolites. Clays and Clay Minerals, 23, 119–124.

Augsburger, M.S., Strasser, E., Perino, E., Mercader, R.C., and Pedregosa, J.C. (1998) FTIR and Mössbauer investigation of a substituted palygorskite: Silicate with a channel structure. Journal of Physics and Chemistry of Solids, 59, 175–180.

Barron, P.F. and Frost, R.L. (1985) Solid-state ^{29}Si NMR examination of the 2:1 ribbon magnesium silicates, sepiolite, and palygorskite. American Mineralogist, 70, 758–766.

Bokobza, L. (2002) Origin of Near-Infrared absorption bands. In H.W. Siesler, Y. Ozaki, S. Kawata, and H.M. Heise, Eds., Near Infrared Spectroscopy: Principles, Instruments, Applications, p. 11–41. Wiley-VCH, Berlin.

Breitinger, D.K., Schukow, H., Betz, H.-H., Mohr, J., and Schwab, R.G. (1999) Two-phonon excitations in the IR and NIR spectra of alunites. Journal of Molecular Structure, 480–481, 677–682.

Bush, S.G., Jorgenson, J.W., Miller, M.L., and Linton, R.W. (1983) Transmission Near-Infrared technique for evaluation and relative quantitation of surface groups on silica. Journal of Chromatography, 260, 1–12.

Chahi, A., Petit, S., and Decarreau A. (2002) Infrared evidence of dioctahedral-trioctahedral site occupancy in palygorskite. Clays and Clay Minerals, 50, 306–313.

Chiari, G., Giustetto, R., and Ricchiardi, G. (2003) Crystal structure refinement of palygorskite and Maya Blue from molecular modeling and powder synchrotron diffraction. European Journal of Mineralogy, 15, 21–33.

Chipera, S.J. and Bish, D.L. (2001) Baseline studies of the Clay Minerals Society Source Clays: Powder X-ray diffraction analyses. Clays and Clay Minerals, 49, 398–409.

Chisholm, J.E. (1992) Powder-diffraction patterns and structural models for palygorskite. Canadian Mineralogist, 30, 61–73.

Clark, R.N., King, T.V.V., Klejwa, M., Swayze, G.A., and Vergo, N. (1990) High spectral resolution reflectance spectroscopy of minerals. Journal of Geophysical Research, 95, 12653–12680.

Farmer, V.C. (1974) The layer silicates. In V.C. Farmer, Ed., The Infrared Spectra of Minerals, p. 331–363. Mineralogical Society Monograph 4, London.

Frost, R.L., Locos, O.B., Ruan, H., and Kloprogge, J.T. (2001) Near-infrared spectroscopic study of sepiolites and palygorskites. Vibrational Spectroscopy, 27, 1–13.

Galán, E. and Carretero, I. (1999) A new approach to compositional limits for sepiolite and palygorskite. Clays and Clay Minerals, 47, 399–409.

Gates, W.P. (2005) Infrared spectroscopy and the chemistry of dioctahedral smectites. In T. Kloprogge, Ed., The Application of Vibrational Spectroscopy to Clay Minerals and Layered Double Hydroxides, 13, p.126–168. CMS Workshop Lectures, The Clay Minerals Society, Chantilly, Virginia.

Gates, W.P., Slade, P.G., Manceau, A., and Lanson, B. (2002) Site occupancies by iron in nontronites. Clays and Clay Minerals, 50, 223–239.

Giustetto, R. and Chiari, G. (2004) Crystal structure refinement of palygorskite from neutron powder diffraction. European Journal of Mineralogy, 16, 521–532.

Goodman, B.A., Russell, J.D., Fraser, A.R., and Woodhams, F.W.D. (1976) A Mössbauer and IR spectroscopic study of the structure of nontronite. Clays and Clay Minerals, 24, 53–59.

Guggenheim, S. and Koster van Groos, A.F. (2001) Baseline studies of the Clay Minerals Society Source Clays: Thermal Analysis. Clays and Clay Minerals, 49, 433–443.

Hayashi, H., Otsuka, R., and Imai, N. (1969) Infrared study of sepiolite and palygorskite on heating. American Mineralogist, 53, 1613–1624.

Kastritis, I.D., Mposkos, E., and Kacandes, G.H. (2003) The palygorskite and Mg-Fe smectite clay deposits of the Ventzia basin, Western Macedonia, Greece. In D. Eliopoulos, et al. Eds., Mineral exploration and sustainable development—Proceedings of the 7th SGA Meeting, p. 891–894. Millpress, Rotterdam.

Khorami, J. and Lemieux, A. (1989) Comparison of attapulgites from different sources using TG/DTG and FTIR. Thermochimica Acta, 138, 97–105.

Kuang, W., Glenn, A.F., and Detellier, C. (2004) Dehydration and rehydration of Palygorskite and the influence of water on the nanopores. Clays and Clay Minerals, 52, 635–642.

Madejová, J. (2003) FTIR techniques in clay mineral studies. Vibrational Spectroscopy, 31, 1–10.

Madejová, J. and Komadel, P. (2001) Baseline studies of the Clay Minerals Society Source Clays: Infrared methods. Clays and Clay Minerals, 49, 410–432.

McKeown, D.A., Post, J.E., and Etz, E.S. (2002) Vibrational analysis of palygorskite and sepiolite. Clays and Clay Minerals, 50, 667–680.

Mehra, O.P. and Jackson, M.L. (1960) Iron oxide removal from soils and clays by a dithionite-citrate system buffered with sodium bicarbonate. Clays and Clay Minerals, 7, 317–327.

Mendelovici, E. (1973) Infrared study of attapulgite and HCl treated attapulgite. Clays and Clay Minerals, 21, 115–119.

Mermut, A.R. and Cano, A.F. (2001) Baseline studies of the Clay Minerals Society Source Clays: Chemical analyses of major elements. Clays and Clay Minerals, 49, 381–386.

Morrow, B.A. and McFarlan, A.J. (1992) Surface vibrational modes of silanol groups on silica. Journal of Physical Chemistry, 96, 1395–1400.

Petit, S., Robert, J.-L., Decarreau, A., Besson, G., Grauby, O., and Martin, F. (1995) Apport des méthodes spectroscopiques à la caractérisation des phyllosilicates 2:1. Bulletin de Centre des Recherches Exploration-Production ELF-Aquitaine, 19, 119–147.

Post, J.L. and Noble, P.N. (1993) The Near-infrared combination band frequencies of dioctahedral smectites, micas, and illites. Clays and Clay Minerals, 41, 639–644.

Prost, R. (1975) Etude de l'hydratation des argiles: interactions eau-mineral et mécanisme de la rétention de l' eau. Ph.D. Thesis, Université Pierre et Marie Curie, Paris VI.

Russell, J.D. and Fraser, A.R. (1994) Infrared methods. In M.J. Wilson, Ed., Clay Mineralogy: Spectroscopic and Chemical Determinative Methods, p. 11–67. Chapman and Hall, London.

Russell, J.D., Farmer, V.C., and Velde, B. (1970) Replacement of OH by OD in layer silicates and identification of the vibrations of these groups in the infrared spectra. Mineralogical Magazine, 37, 869–879.

Serna, C., Ahlrichs, J.L., and Serratosa, J.M. (1975) Folding in Sepiolite crystals. Clays and Clay Minerals, 23, 452–457.

Serna, C., VanScoyoc, G.E., and Ahlrichs, J.L. (1977) Hydroxyl groups and water in palygorskite. American Mineralogist, 62, 784–792.

Singer, A. (1989) Palygorskite and Sepiolite Group Minerals. In J.B. Dixon and S.B. Weed, Eds., Minerals in Soil Environments, 1, Ch. 17, p. 829–872. SSSA Book Series, Soil Science Society of America, Madison, Wisconsin.

Szekeres, M., Kamalin, O., Grobet, P.G., Schoonheydt, R.A., Wostyn, K., Clays, K., Persoons, A., and Dékány, I. (2003) Two-dimensional ordering of Stöber silica particles at the air/water interface. Colloids and Surfaces A: Physicochemical and Engineering Aspects, 227, 77–83.

Tarte, P., Pottier, M.J., and Procès, A.M. (1973) Vibrational studies of silicates and germinates—V. IR and Raman spectra of pyrosilicates and pyrogermanates with a linear bridge. Spectrochimica Acta, 29A, 1017–1027.

VanScoyoc, G.E., Serna, C.J., and Ahlrichs, J.L. (1979) Structural changes in palygorskite during dehydration and dehydroxylation. American Mineralogist, 64, 215–223.

Weckler, B. and Lutz, H.D. (1996) Near-infrared spectra of M(OH)Cl (M=Ca, Cd, Sr), Zn(OH)F, γ-$Cd(OH)_2$, $Sr(OH)_2$, and brucite-type hydroxides $M(OH)_2$ (M=Mg, Ca, Mn, Fe, Co, Ni, Cd). Spectrochimica Acta A, 52, 1507–1513.

Yuan, P., Wu, D.Q., He, H.P., and Lin, Z.Y. (2004) The hydroxyl species and acid sites on diatomite surface: a combined IR and Raman study. Applied Surface Science, 227, 30–39.

Zviagina, B.B., McCarty, D.K., Środoń, J., and Drits, V.A. (2004) Interpretation of infrared spectra of dioctahedral smectites in the region of OH-stretching vibrations. Clays and Clay Minerals, 52, 399–410.

MANUSCRIPT RECEIVED JUNE 30, 2005
MANUSCRIPT ACCEPTED FEBRUARY 6, 2006
MANUSCRIPT HANDLED BY STEPHEN GUGGENHEIM